

Portable Adaptive Optics for exoplanet imaging *

Yong-Tian Zhu^{1,2}, Jiang-Pei Dou^{*1,2}, Xi Zhang^{1,2}, Gang Zhao^{1,2}, Jing Guo^{1,2}, Leopoldo Infante^{3,4}

¹ National Astronomical Observatories / Nanjing Institute of Astronomical Optics & Technology, Chinese Academy of Sciences, Nanjing 210042, China ; jpdou@niaot.ac.cn

² Key Laboratory of Astronomical Optics & Technology, Nanjing Institute of Astronomical Optics & Technology, Chinese Academy of Sciences, Nanjing 210042, China

³ Las Campanas Observatory Carnegie Institution of Washington, Colina El Pino Casilla 601 La Serena, Chile

⁴ Institute of Astrophysics, Pontificia Universidad Católica de Chile, Av. Vic Mackenna 4860, Santiago, Chile

Received 20XX Month Day; accepted 20XX Month Day

Abstract The Portable Adaptive Optics (PAO) is a low-cost and compact system, designed for 4-meter class telescopes that have no Adaptive Optics (AO), because of the physical space limitation at the Nasmyth or Cassegrain focus and the historically high cost of the conventional AO. The initial scientific observations of the PAO are focused on the direct imaging of exoplanets and sub-stellar companions. This paper discusses the PAO concept and the associated high-contrast imaging performance in our recent observational runs. PAO is delivering a Strehl ratio better than 60% in H band under median seeing conditions of $1''$. Combined with our dedicated image rotation and subtraction (IRS) technique and the optimized IRS (O-IRS) algorithm, the averaged contrast ratio for a $5 \leq V_{\text{mag}} \leq 9$ primary star is 1.3×10^{-5} and 3.3×10^{-6} at angular distance of $0.36''$ under exposure time of 7 minutes and 2 hours, respectively. PAO has successfully revealed the known exoplanet of κ And b, in our recent observation at 3.5-meter ARC telescope at Apache Point Observatory. We have performed the associated astrometry and photometry analysis of the recovered κ And b planet, which gives a projected separation of $0.984 \pm 0.05''$, a position angle of $51.1 \pm 0.5^\circ$, and a mass of $10.15^{+2.19}_{-1.255} M_{\text{Jup}}$. These results demonstrate that PAO can be used for direct imaging of exoplanets with medium-sized telescopes.

Key words: stars: imaging — instrumentation: adaptive optics — instrumentation: high angular resolution — methods: observational — techniques: image processing

1 INTRODUCTION

With over 3800 already known exoplanets, most of them were discovered by the indirect detection approaches including transit and radial velocity. However, the direct imaging method has become increasingly important, since it can spatially separate the light of a planet from the host star. It has opened a window for the spectroscopy analysis of the atmosphere of the planet, thus will eventually allow the detection of terrestrial biology signals in future space missions. With high-contrast imaging technique,

* Supported by the National Natural Science Foundation of China.

several giant planets have been detected at relatively large orbital separations by ground-based observations (Macintosh et al. 2015). The HR 8799 system with four giant planets, for instance, have been observed and recovered mostly by current 8-10 meter class telescopes (Marois et al. 2008, 2010). The existence of giant planets at large angular separations has challenged the current planet formation model. However, the amount of exoplanets detected by direct imaging is still low comparing with other indirect detection approaches, it therefore requires more high-contrast imaging instruments and the associated scientific observations on as many telescopes as possible, including those small-size telescopes with 2-4 meter aperture.

Most of the discovered exoplanets through direct imaging are, in general, young and self-luminous, and have large orbit separations, which makes them possible to be imaged in infrared and resolved with small telescopes. The observation with small-size telescope has fully demonstrated in Serabyn et al (2010) work. With a 1.5-meter resultant aperture telescope, three of the HR 8799 exoplanets were also recovered by using extreme adaptive optics system that delivers a Strehl ratio of 0.91 at the NIR K band (Serabyn et al. 2010). The high-contrast imaging with small telescopes would be especially important for these time-intensive surveys (Mawet et al. 2009).

We have proposed and built the first PAO that is optimized for exoplanets high-contrast imaging with current 2-4 meter class telescopes since 2013. By employing small-aperture deformable mirror (DM) with micro-electro-mechanical systems (MEMS) technique and the rapid programming of LabVIEW based control software, the PAO features a compact physical size, low cost, high performance and high flexibility that makes it is able to work with any size of telescopes. The PAO with a "small" telescope can provide a high Strehl ratio, since a DM with moderate actuator number can be used and AO high speed correction is achievable.

One of the critical issue for exoplanet high-contrast imaging is the so called non-common path aberrations (NCPA). Both GPI and SPHERE use the two-step approach, which requires a post calibration interferometer or the phase-diversity algorithm to measure the differential aberration then command the DM to correct it (Hinkley et al. 2009; Fusco et al. 2006; Sauvage et al. 2007). In 2012, we presented a unique technique that uses the focal plane PSF information to directly command the DM to correct the NCPA, which was based on an iterative optimization algorithm (Dou et al. 2011; Ren et al. 2012a). The approach can correct the differential aberration in a single step, which has locked on a wave front with accuracy on the order of 7.4×10^{-4} wavelengths.

PAO as a visiting instrument has been used at ESO's 3.6-meter NTT and the 3.5-meter ARC telescope in Apache Point Observatory. In recent observation, PAO has successfully recovered the known exoplanet of κ And b under a medium seeing condition. With O-IRS reduction, it has delivered a contrast ratio of 1.3×10^{-5} and 3.3×10^{-6} at angular distance of $0.36''$ under exposure time of 7 minutes and 2 hours, respectively.

In this paper, we present the development and performance of PAO during recent observations. In Section 2, we review the development history of PAO; In Section 3, we describe the design and associated performance of PAO and provide the observation results especially the analysis of the recovered planet of κ And b; conclusions and future work will be presented in Section 4.

2 PAO HISTORY

PAO is a nighttime AO system that is originated from the Portable Solar Adaptive Optics (PSAO). PSAO is initially proposed for diffraction-limited imaging of the Sun (Ren et al. 2009). PSAO has been fully tested with different solar telescopes at different seeing conditions, in which it can always be able to deliver good performance (Ren et al. 2010; 2012; 2012a; Ren & Zhu 2013).

We then developed PAO from PSAO by simply replacing the cross-correlation module for daytime wave-front sensing into the centroid-calculation module for nighttime wave-front sensing. The first PAO test observation was conducted in 2013, in which the white dwarf Sirius B in a binary system has been clearly imaged, at NSO's 1.6-meter McMP solar telescope (Ren et al. 2014).

PAO was then updated and firstly optimized for 4-meter class telescope for more experimental observations since 2014. The PAO prototype system has employed a DM with 97 actuators. With $9 \times$

9 wave-front sensor (WFS) sub-apertures, PAO can stably work with a correction speed at 1000 Hz. The first engineering observation was carried out at ESO 3.6-meter NTT telescope in Chile in July, 2014. Six nights was approved by ESO and the observation program was under collaboration with the collaboration of Pontificia Universidad Católica de Chile, with the support of Chinese Academy of Sciences South America Center for Astronomy (CASSACA). But due to strong wind on the site, only 3 nights were actually allowed to be used during our 6-night observation run, however it was the first time to show our PAO is able to rapidly connect with 4-meter class telescope and provide effective corrections.

Figure 1 shows 3.6-meter NTT telescope (left panel) and our PAO interfaced with the telescope Nasmyth B port (right panel).

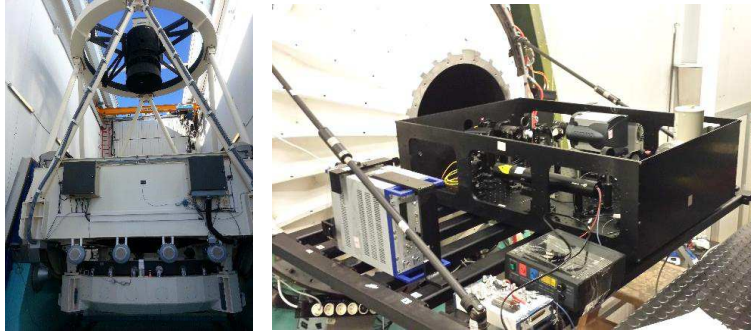


Fig. 1: The 3.6-meter NTT telescope and PAO installed on NB.

Figure 2 shows an example of a PSF before AO correction (panel a), after AO correction (panel b), and finally processed with O-IRS (panel c). The achieved contrast are shown in panel d). Here we use 144 frames with each frame under a 3 seconds exposure time, which gives a 7 minutes integration time in total. The blue, red and green lines correspond to the direct combination, LOCI (Lafrenière et al. 2007) and O-IRS reduction (Ren et al. 2012b; Dou et al. 2015). An initial contrast ratio on the order of 10^{-4} has achieved at an angular separation of $0.5''$. The above engineering observation clearly demonstrated the feasibility of our PAO technique.

3 PAO DESCRIPTION

After fully demonstration that the PAO can be used for scientific exoplanet imaging, we purchased more observational time of the 3.5-meter ARC telescope, with the goal to further explore and improve the PAO's capabilities for exoplanet imaging.

3.1 Optics layout and expected performance

To further improve the high contrast performance, PAO was finally updated and optimized for the 3.5-meter ARC telescope in Apache Point Observatory located in US. Figure 3 shows the optics layout of the PAO for the 3.5-meter ARC telescope. The light from the telescope focus TF (F/# 10.35) is collimated by the cemented doublet lens with a focal length of 150 mm, in order to match the clear aperture of the DM of 13.5 mm. The tip-tilt mirror (TTM) is located behind the collimator for overall tip-tilt correction. The light propagates to the DM, which corrects possible wave-front errors. A dichroic beam-splitter (BS) is located behind the DM. The visible light is reflected by the beam-splitter to the WFS for wave-front sensing, while the infrared light continuously propagates to a science near infrared (NIR) camera, where the high-contrast image is formed on the focal plane IM at f/50 by the Imaging Lens. The whole PAO system was built on a $0.9 \times 0.78 \times 0.3 \text{ m}^3$ self-containing enclosed box that will be installed on the ARC Nasmyth A Port.

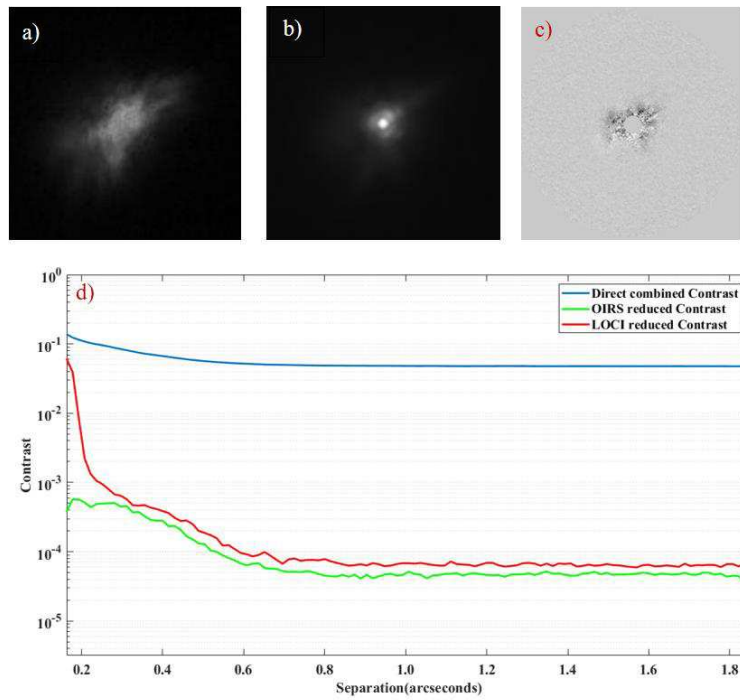


Fig. 2: An example of high-contrast reduction for H band observation of Star Fomalhaut.

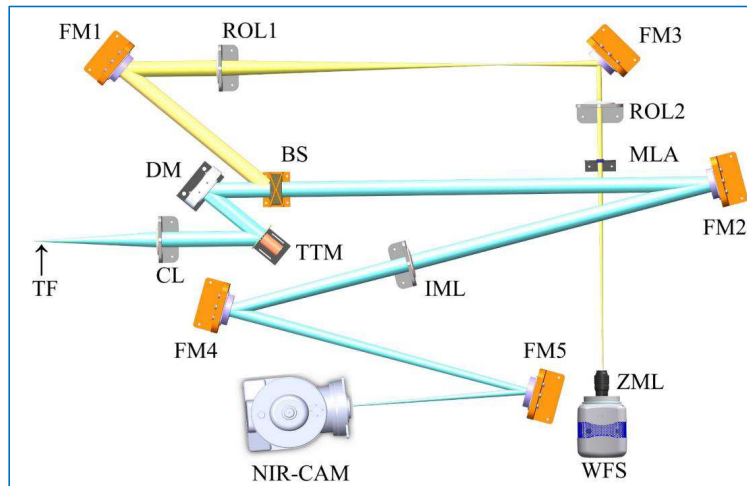


Fig. 3: Optics layout of PAO optimized for exoplanet scientific observation.

Employing a high speed 97-element DM and an EMCCD as the WFS camera, PAO could achieve the maximum speed of 1300 Hz for open-loop correction. Table 1 lists the PAO specifications and estimated performances. The PAO used the DM-97 with a correction speed increased to 2000 Hz, with $10\text{-}\mu\text{m}$ wave-front stroke. The tip/tilt mirror is mounted on the PI's S-330.4SL piezo tip/tilt platform. The optical deflection angle in the 2 orthogonal axes is 10 mrad and the tilt/tilt platform can achieve a resonance frequency of about 1600 Hz (loaded). The WFS has 9×9 sub-apertures (excluding those in the 4 corners), each sub-aperture will be sampled by 4×4 pixels on the WFS camera. The WFS camera

is an EMCCD purchased from Photometrics. It has 512×512 pixels ($16 \times 16 \mu\text{m}$ pixel size), with less than $1e^-$ readout noise in EM gain mode, and can deliver a frame rate of 1820 Hz for our PAO with a region of 64×64 pixels. The science camera is a NIR camera from Xenics.

Table 1: AO Hardware specifications and performance for bright NGSs at good seeing $r_0 = 13$ cm.

Hardware	Specifications
DM	97 actuators in 10×10 configuration, $\pm 5\text{-}\mu\text{m}$ wave-front stroke, 13.5-mm clear aperture, 2000 Hz frame rate
TTM	PI S-330.4SL, 5 mrad stroke range, 1600 Hz frame rate
WFS	9×9 Shack-Hartmann sub-apertures, 4×4 pixels / sub-aperture
WFS camera	Photometrics Evolve-512 Delta EMCCD, 1820 Hz at 64×64 pixels
AO correction speed	1300 Hz
Computer	4×12 -core Intel Xeon [®] E5-4657L v2 2.4 GHz (48 cores total)
Field of view	$30'' \times 30''$
Strehl ratio at $m_v = 5$	0.64 at H
Strehl ratio at $m_v = 10$	0.52 at H

The error budget of our AO with the SH WFS can be calculated as the residual variance

$$\sigma^2 = \sigma_{fit}^2 + \sigma_r^2 + \sigma_{ph}^2 + \sigma_{bw}^2, \quad (1)$$

where σ_{fit}^2 is the fitting error that represents the wave-front variance due to the limited DM actuator number comparing to the telescope aperture, σ_r^2 is WFS read noise error, σ_{ph}^2 is the photon noise error, σ_{bw}^2 is the lag error due to finite AO bandwidth. The fitting error is determined by the actuator number which is 97. The read noise is determined by the WFS camera readout noise which is ($0.15e^-$). The photon noise is determined by the NGS magnitude and sub-aperture size. The lag error is determined by the AO correction speed which is 1300 Hz and average wind speed which is 20 m/s. For small residual variance, the Strehl ratio can be calculated by using the analytical equation $S = \exp(-\sigma^2)$. To precisely evaluate the above errors, it depends on many factors including seeing parameter r_0 , NGS brightness, telescope aperture size and its central obstruction, sub-aperture number of SH WFS, as well as the telescope and SH WFS/DM geometric configurations and other properties, which refer to complicate analytical process. Here we calculate the Strehl ratios (SR) using the end-to-end software YAO simulation software package (<http://frigaut.github.io/yao/>), with all above error sources and configurations inputted (fitting error, read noise, photon noise, bandwidth, telescope and WFS/DM geometric configurations etc.), and this yields more realistic results. Figure 4 shows the interface of the YAO software for the simulation of PAO correction of bright stars. Since the non-common-path error will be corrected by our SPGD algorithm, it is not included in the above calculation/simulation. The AO performance is a function of the seeing condition as well as the guide star brightness. At the good seeing $r_0 = 13$ cm at 500-nm, the Strehl ratio is 0.64 at the H ($1.60\text{-}\mu\text{m}$) band, for a natural guide star with $m_v = 5$, as shown in Table 1 and Figure 5. The AO should deliver better performances at excellent seeing conditions.

The simulation software YAO can calculate the PAO instant PSF. The AO corrected PSFs are variable with a period of speckle life t_0 , which is determined as $t_0 = 0.6D/v$ (Macintosh et al. 2005), where D is telescope aperture diameter and v is the atmosphere wind speed. For an AO system with the NCPA corrected, the contrast can be improved by increasing the exposure time, with improving factor as \sqrt{T}/t_0 , where T is the exposure time. Figure 6 shows the expected achievable contrast for the H band exoplanet imaging with $m_v = 5$ NGS with an exposure time of 1 hour and 4 hours, respectively. This is achieved by using our unique O-IRS reduced of all instant PSFs, each with an exposure of speckle life (Dou et al. 2015). The simulation results prove that the PAO can deliver a contrast $10^{-5.7}$ and 10^{-6} at an angular separation of $1''$, for an exposure of 1 hour and 4 hours respectively.

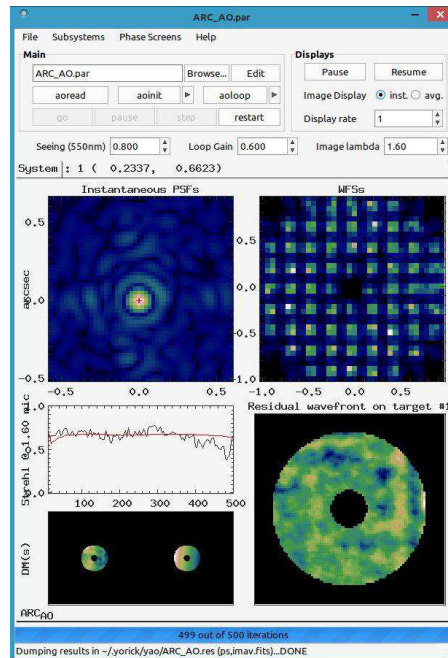


Fig. 4: YAO interface for PAO performance simulation.

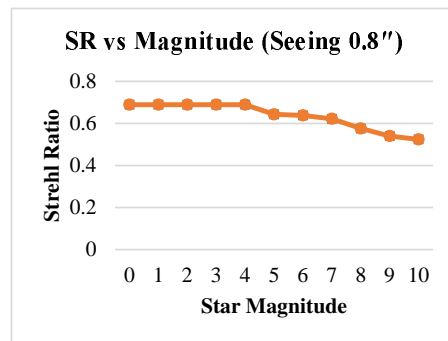


Fig. 5: Expected SR correction performance of PAO for different magnitude stars.

3.2 PAO Performance at 3.5-meter ARC Telescope

3.2.1 Observation of the binary stars HR 6212 A and B

Six observation runs have been conducted at 3.5-meter ARC telescope in Apache Point Observatory during 2015 to 2018. Figure 7 shows the 3.5-meter ARC telescope (left panel) and our PAO interfaced with the telescope Nasmyth port (right panel).

The first two runs was carried out in 2015. A couple of targets were used to test PAO potential performance for high-contrast imaging. Figure 8 shows the AO on and off correction of the binary stars HR 6212 A and B, in which the companion star B was clearly shown after PAO correction. Figure 9 shows the associated contrast achieved with the APO 3.5-meter telescope with an exposure of 7 minutes after O-IRS data reduction. A contrast of 1.3×10^{-5} was achieved at an inner working angle (IWA) of $0.36''$, corresponding to $4\lambda/D$, four times of the coronagraph diffraction beam, which implies that the

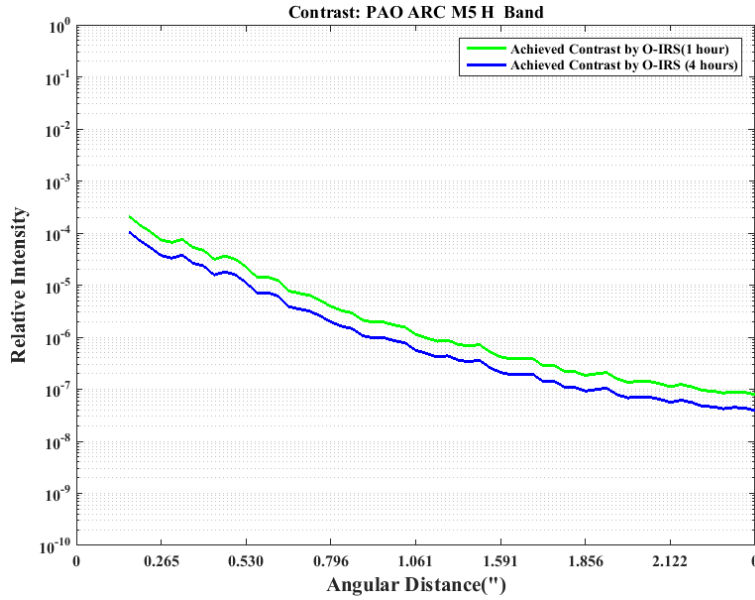


Fig. 6: Expected contrast performance of PAO for $M_v = 5$ star at H band.

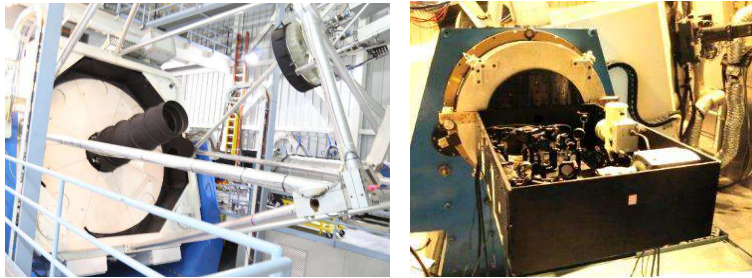


Fig. 7: The 3.5-meter ARC telescope and the PAO installed on NA2.

contrast of 3.3×10^{-6} should be achievable with a longer exposure time of 2 hours. The Extreme AOs in routine operation such as GPI and SPHERE on 8-meter telescopes has better performance than current PAO, which can deliver better imaging contrasts of 10^{-6} from the angular distance of $0.3''$, considering the Extreme AOs use denser sub-apertures to sample the telescope pupil. However the PAO still showed its capability of imaging exoplanets and brown dwarfs on middle-sized telescopes. The data reduction was conducted by using our O-IRS algorithm (Dou et al. 2015). This result clearly indicates that our portable adaptive optics is a mature technique and is ready to be used for scientific exoplanet imaging.

3.2.2 Observation of the known exoplanet κ And b

We firstly conducted the high-contrast imaging observation of κ And b in 2014 in H -band at 3.5-meter ARC in APO Observatory to testify PAO's capability of direct imaging of giant exoplanets around young stars. The planet κ And b was firstly imaged in 2012 by using the Subaru/HiCIAO during the SEEDS survey (Carson et al. 2013) and then characterized by the subsequent New Keck and LBTI high-contrast observations in 2012 and 2013 (Bonnetfoy et al. 2014). These observations were carried out in J , H , K_s

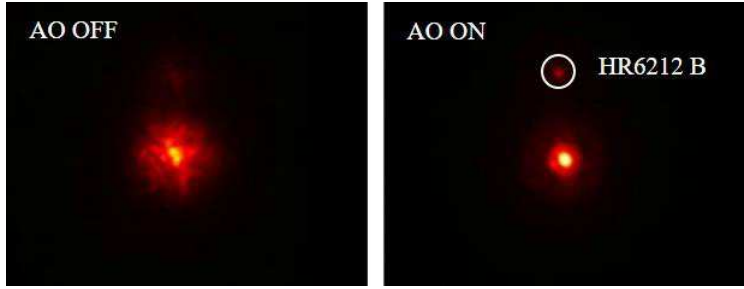


Fig. 8: HR 6212 A/B images before and after PAO correction at 3.5-meter ARC telescope.

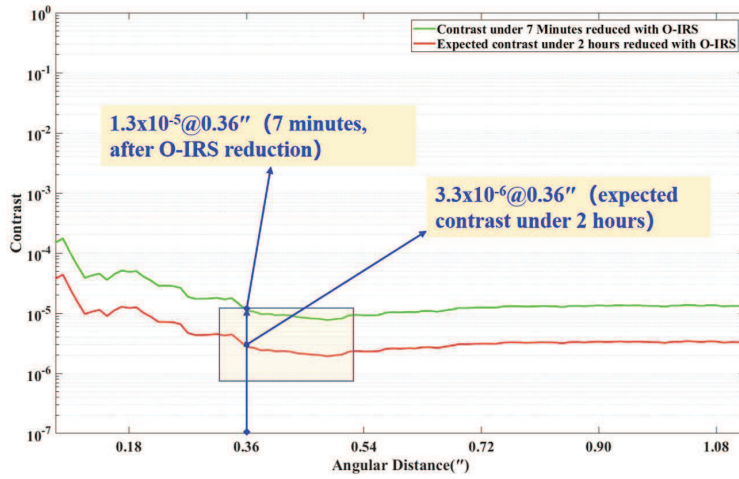


Fig. 9: Contrast achieved with PAO at 3.5-meter ARC telescope.

and L_p infrared bands respectively. For our current NIR camera is cut-off at $1.55 \mu\text{m}$, in this observation run, we only take the H band data for demonstration purpose.

The observation was carried out with the NIR camera using the 640×512 pixels array and under the angular differential imaging (ADI) mode without any field rotation compensation. All frames of the host star κ And were acquired under 2 seconds exposure time without saturation for the following photometric measurement to derive the flux ratios, in order to compare this observation result with the previous ones. The data were saved in a cube with 50 frames in each cube and 23 cubes in total. The integration time of all cubes were 2300 s with a small field rotation of 8.83 degrees. Figure 10 shows one single frame image of κ And after PAO correction.

3.3 Data reduction

The raw images were processed based on our recently developed data reduction pipeline for high contrast imaging (Dou et al. 2015). We firstly carried out the basic reduction including bad pixels and cosmic rays, dark current, flat field and background calibrations; then these images were registered and conducted the speckle suppression based on O-IRS and PCA, respectively (Ren et al. 2012b; Dou et al. 2015; Amara & Quanz 2012; Otten et al. 2017). The pipeline is written in both IDL and Python, a well-known and frequently used language in astronomical environments.

Meanwhile, we performed the astrometry analysis of the planet b, in which we took into account the positional uncertainties of the centroid errors of the companion, and systematic errors in the distortion

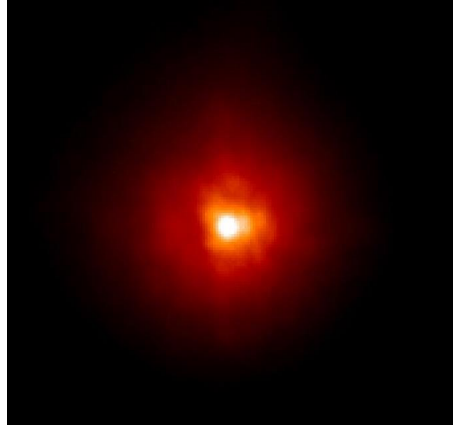


Fig. 10: The observed κ And image after PAO correction under seeing of $1''$.

solution and the north/west alignment. For the orientation alignment, we have recorded two cubes of images when moving the telescope toward north (distance of $2.7''$) firstly then to the east (distance of $2.9''$), respectively. The image rotation angle was calculated by using the center of the median of all images in the two cubes, which gives a rotation angle of $4.5 \pm 0.5^\circ$ to align the north orientation with the y axis of the image. And the pixel scale of PAO image is found out to be $0.024''/\text{pixel}$. Finally, the reduced image of κ And b processed by the PCA-based algorithm was de-rotated of 4.5° and shown in Figure 11. Table 2 listed the astrometry analysis results based on previous observation in 2012-2013 and in this observation.

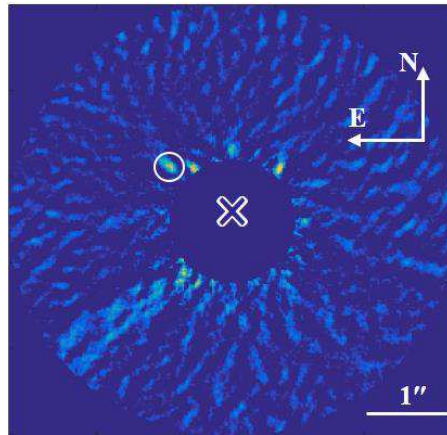


Fig. 11: The reduced image of planet κ And b, the star center is marked with cross.

We then performed the photometry analysis of the reduced planets. A series of artificial planets were added in the same data of κ And after basic reduction with a certain contrast, with a similar procedure that has been used in previous work (Lafrenière et al. 2007; Dou et al. 2015). In each frame of the data set, planets are inserted at eleven different azimuth angles. In order to cover the region where planet b is located, here several artificial planets along one radius were added, in which the second innermost one has an angular separation of $0.984''$, the same as planet b. The final frame has a field rotation of 8.83 degrees, which is also the same as the data set. Then the speckle suppression based on O-IRS and PCA are carried on these images in the data set, respectively. Figure 12 shows the reduced image with artificial planets by using the PCA-based algorithms, when adjusting the intensity of the artificial planet

Table 2: Astrometry analysis of planet κ And b.

Date	<i>H</i> band (1.63 μm)		<i>K_s</i> (2.65 μm)		<i>H</i> band (1.55 μm)	
	Proj. sep. (")	Proj. ang. (")	Proj. sep. (")	Proj. ang. (")	Proj. sep. (")	Proj. ang. (")
2012 January 1	1.070 ± 0.010	55.7 ± 0.6				
2012 July 8	1.058 ± 0.007	56.0 ± 0.4				
2012 October 30			1.029 ± 0.005	55.3 ± 0.3		
2012 November 3						
2017 June 10					0.984 ± 0.05	51.1 ± 0.5
Reference	(1)		(2)		(3)	

Notes: References: (1) [Carson et al. 2013](#); (2) [Bonnefoy et al. 2014](#); (3) this work.

to be the same as the planet b. It finally gives a contrast of $4.691 \pm 0.85 \times 10^{-5}$, which corresponding to the magnitude of 15.145 ± 0.195 at $1.55 \mu\text{m}$. In Figure 12, an annulus between $0.895''$ and $1.072''$ has added to cover the location of planet κ And b. The signal to noise ratio (S/N) of the planet has been calculated, which is 7.75σ .

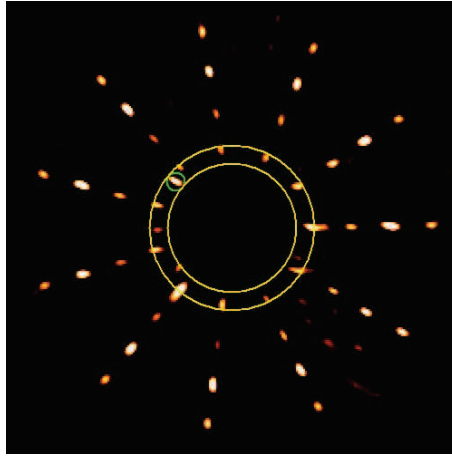


Fig. 12: The reduced image of κ And with artificial planets added: the location of planets b is marked in the green circle, while the yellow annulus shows the second innermost artificial planets with the same angular separation of planet b.

A summary of the available photometry is presented in Table 3. Here we employ the same physical parameters of the primary star of κ And b as the work in [Carson et al. 2013](#), in which the estimated age is 30_{-10}^{+20} Myr, and the parallax is 19.2 ± 0.7 ([Perryman et al. 1997](#)). The *H*-band ($1.55 \mu\text{m}$) magnitude is 15.145 ± 0.195 gives a mass of $10.15_{-1.255}^{+2.19} M_{\text{Jup}}$ and a temperature of $1227_{-4.5}^{+4}$ K by employing the BT-DUSTY evolutionary models ([Chabrier & Baraffe 2000](#); [Spiegel & Burrows 2012](#)).

Table 3: Photometry analysis of planet κ And b.

Planets	<i>J</i> band (1.25 μm)	<i>H</i> band (1.63 μm)	<i>H</i> band (1.55 μm)	<i>K_s</i> (2.65 μm)	<i>L'</i> (3.8 μm)	<i>NB</i> (4.05 μm)	<i>M</i> (4.7 μm)
κ And b	15.86 ± 0.21 16.3 ± 0.3	14.95 ± 0.13 15.2 ± 0.2	15.145 ± 0.195	14.32 ± 0.09 14.6 ± 0.4	13.12 ± 0.1 13.12 ± 0.09	13.0 ± 0.2	13.3 ± 0.3
Reference	(1), (2)	(1), (2)	(3)	(1), (2)	(1), (2)	(1)	(1)

Notes: References: (1) [Bonnefoy et al. 2014](#); (2) [Carson et al. 2013](#); (3) this work.

4 CONCLUSIONS

In this paper, we have briefly reviewed the development history of PAO technique. We then update the PAO to be a visiting instrument that is optimized for the direct imaging of exoplanets and sub-stellar companions. The unique feature of PAO with a compact physical size and high performance allows it to be used at current 3-4 meter class telescopes. In the most recent observation at 3.5-meter ARC telescope at APO, we have successfully recovered the known exoplanet of κ And b reduced by using our unique O-IRS and PCA algorithm, respectively. The observation contrast has reached 10^{-5} at an angular distance from $0.36''$ to $1''$. Finally, we have performed the associated astrometry and photometry analysis of the recovered κ And b planet, which is consistent with the previous work. It has fully demonstrated that our portable high-contrast imaging system can be used for the exoplanets direct imaging observation with middle-class telescopes.

Acknowledgements Y.-T. Zhu acknowledges the support from the National Natural Science Foundation of China (NSFC) under grant # 11827804. J.-P. Dou acknowledges the support from the National Natural Science Foundation of China (NSFC) under grant # U2031210.

References

- Amara, A., & Quanz, S. P. 2012, MNRAS, 427, 948 [8](#)
- Bonnefoy, M., Currie, T., Marleau, G. D., et al. 2014, A&A, 562, A111 [7](#), [10](#)
- Carson, J., Thalmann, C., Janson, M., et al. 2013, ApJ, 763, L32 [7](#), [10](#)
- Chabrier, G., & Baraffe, I. 2000, ARA&A, 38, 337 [10](#)
- Dou, J.-P., Ren, D.-Q., & Zhu, Y.-T. 2011, Research in Astron. Astrophys. (RAA), 11, 198 [2](#)
- Dou, J., Ren, D., Zhao, G., et al. 2015, ApJ, 802, 12 [3](#), [5](#), [7](#), [8](#), [9](#)
- Fusco, T., Petit, C., Rousset, G., et al. 2006, in Proc. SPIE, Vol. 6272, 62720K [2](#)
- Hinkley, S., Oppenheimer, B. R., Soummer, R., et al. 2009, ApJ, 701, 804 [2](#)
- Lafrenière, D., Marois, C., Doyon, R., Nadeau, D., & Artigau, É. 2007, ApJ, 660, 770 [3](#), [9](#)
- Macintosh, B., Poyneer, L., Sivaramakrishnan, A., & Marois, C. 2005, in Proc. SPIE, Vol. 5903, 59030J [5](#)
- Macintosh, B., Graham, J., Barman, T., et al. 2015, Science, 350, 64 [2](#)
- Marois, C., Macintosh, B., Barman, T., et al. 2008, Science, 322, 1348 [2](#)
- Marois, C., Zuckerman, B., Konopacky, Q. M., Macintosh, B., & Barman, T. 2010, Nature, 468, 1080 [2](#)
- Mawet, D., Serabyn, E., Stapelfeldt, K., & Crepp, J. 2009, ApJ, 702, L47 [2](#)
- Otten, G. P. P. L., Snik, F., Kenworthy, M. A., et al. 2017, ApJ, 834, 175 [8](#)
- Perryman, M. A. C., Lindegren, L., Kovalevsky, J., et al. 1997, A&A, 323, L49 [10](#)
- Ren, D., & Dong, B. 2012, Opt. Eng., 51, 101705 [2](#)
- Ren, D., Dong, B., Zhu, Y., & Christian, D. J. 2012a, PASP, 124, 247 [2](#)
- Ren, D., Dou, J., Zhang, X., & Zhu, Y. 2012b, ApJ, 753, 99 [3](#), [8](#)
- Ren, D., Penn, M., Plymate, C., et al. 2010, in Proc. SPIE, Vol. 7736, 77363P [2](#)
- Ren, D., Penn, M., Wang, H., Chapman, G., & Plymate, C. 2009, in Proc. SPIE, Vol. 7438, 74380P [2](#)
- Ren, D., & Zhu, Y. 2013, in Adaptive Optics Progress, ed. R. K. Tyson (Rijeka: IntechOpen) [2](#)
- Ren, D., Li, R., Zhang, X., et al. 2014, in Proc. SPIE, Vol. 9148, 91482W [2](#)
- Sauvage, J.-F., Fusco, T., Rousset, G., & Petit, C. 2007, J. Opt. Soc. Am. A, 24, 2334 [2](#)
- Serabyn, E., Mawet, D., & Burruss, R. 2010, Nature, 464, 1018 [2](#)
- Spiegel, D. S., & Burrows, A. 2012, ApJ, 745, 174 [10](#)